False-Alarm Reduction for Low-Frequency Active Sonar With BPSK Pulses: Experimental Results

Mathieu E. G. D. Colin and S. Peter Beerens

***Abstract*—In the last two decades, low-frequency active sonar (LFAS) emerged as one of the most efficient tools for shallow-water antisubmarine warfare (ASW). Like any long-range active sonar system, LFAS produces a large amount of unwanted sea bottom echoes or clutter. These echoes give way to false alarms that increase the computational load of target trackers and delay the correct classification of each echo. The number of false alarms due to clutter can be reduced either through echo classification techniques or through Doppler filtering provided the targets of interest have a nonzero radial velocity. Much research has been carried out on waveform investigation for the efficient use of bandwidth capabilities of modern sonar transmitters. Among the quantity of waveforms, binary phase-shift keyed (BPSK) pulses have emerged as exhibiting cross-correlation properties relevant to Doppler filtering while maintaining a range resolution comparable to frequency-modulated (FM) pulses. In this paper, we have successfully applied a false-alarm reduction technique using contacts obtained with an FM pulse subsequently processed by Doppler filtering with a BPSK pulse. The Doppler filtering performance for this pulse is evaluated on an experimental data set and a few limitations of BPSK are identified.**

***Index Terms*—Phase-shift keying, signal processing algorithms, sonar applications.**

I. Introduction

With the proliferation of smaller and quieter diesel-electric submarines, antisubmarine warfare (ASW) in shallow waters with active hull-mounted and passive towed sonars has become increasingly difficult. However, with the recent introduction of a next generation of sonar, the low-frequency active sonar (LFAS) systems [1], [2], long-range detection of submarines has become feasible. These relatively new systems combine the benefits of current passive systems (low frequencies and the possibility to tow at favorable depth) with those of active systems (independent of the enemy's radiated noise). The first LFAS systems have become operational in the last couple of years. Although performing much better than their predecessors, the shallow-water performance of LFAS can still be improved. The main problem in shallow-water environments is the excessive false-alarm rate. The sonar, designed to detect objects in the water column at long ranges, will not only detect submarines, but also objects on the bottom such as stones, wrecks, and pipelines as well as objects in the water column and at the surface such as drifting containers, fish, whales, or buoys.

A solution to reduce the amount of false alarms while maintaining the system detection capability can be found in the analysis of contact consistency over time and its kinematics. Of all the contacts detected by the system, the most likely to be in motion is an underwater craft, while any strong scatterer lying on the sea bottom will remain still by definition. When Doppler-insensitive pulses such has hyperbolic frequency-modulated (HFM) pulses are used, the kinematics of each persistent contact are often estimated by means of multiple target tracking [3], [4]. However, an excessive quantity of contacts, mostly due to clutter, will build up a heavy load for the tracker. False alarms will lead to false associations, and therefore, not only increase the chance of producing false tracks, but also reduce the probability of constructing a true track. Ideally, as many false alarms as possible should be removed before tracking.

A method contributing to the reduction of false alarm consists of analyzing relevant features of HFM echoes (such as shape or total energy) and applying a classifier to these features [5].

Another method that can be used as a complementary and independent classification technique consists of estimating the range rate of each detected scatterer by measuring the Doppler shift of its echo [6], [7]. The measured Doppler can be either used as an input to the tracker, or used to remove nonmoving contacts, at the risk of losing detections of targets exhibiting no radial velocity. This approach requires the sonar to transmit a Doppler-sensitive waveform. The standard Doppler-sensitive pulse used in active sonar applications is the continuous-wave (CW) pulse [8, p. 194]. It offers an optimal Doppler resolution for a given pulse length, but its range resolution and accuracy make the unambiguous association of CW contacts with HFM contacts challenging. Fusion schemes of HFM and CW contacts have been proposed in [9] and [10]. These studies show the added value of using a combination of linear frequency-modulated (LFM) and CW pulses for both detection and estimation of the sources parameters.

Binary phase-shift keyed (BPSK) pulses offer both Doppler and range resolution and are therefore well suited for contact association. The useful resolution properties of BPSK come at an expense; the sidelobes both in range and in Doppler response are relatively high, making detection difficult in areas with clutter. However, an operational mode with HFM pulses for detection in combination with BPSK for classification seems worthwhile.

In this paper, we first consider a few Doppler-sensitive waveforms and discuss the properties of the BPSK pulse in detail.

Manuscript received November 23, 2009; revised June 28, 2010; accepted November 16, 2010. Date of current version March 18, 2011. This work was supported by the Defence Materiel Organization of The Netherlands.

Associate Editor: D. A. Abraham.

M. E. G. D. Colin is with TNO, The Hague 2509 JG, The Netherlands and also with the Faculty of Aerospace Engineering, Delft University of Technology, Delft 2629 HS, The Netherlands (e-mail: mathieucolin@yahoo.fr).

S. P. Beerens is with TNO, The Hague 2509 JG, The Netherlands.

Color versions of one or more of the figures in this paper are available online at http://ieeexplore.ieee.org.

Digital Object Identifier 10.1109/JOE.2010.2094770

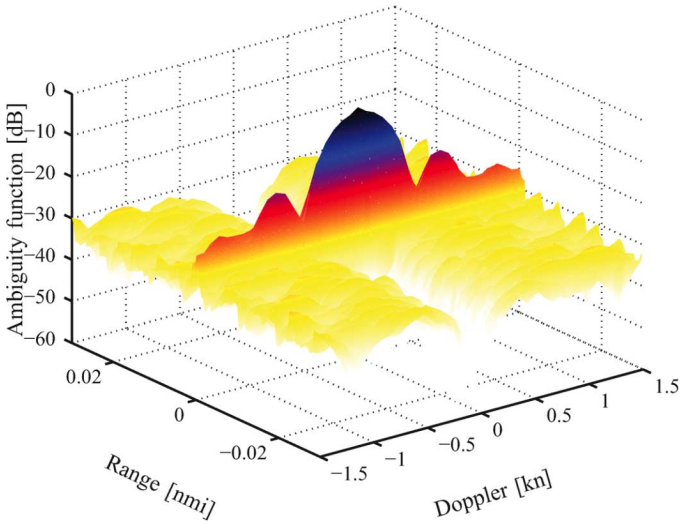

Fig. 1. Theoretical wideband ambiguity surface (range/Doppler plot) of a typical LFAS BPSK pulse (2047-b, 480-Hz bandwidth and 4-s pulse length).

The influence of Doppler spread on BPSK performance is then evaluated. An experiment at sea is then presented and its results are analyzed and interpreted.

II. Doppler-Sensitive Waveforms

The resolution, accuracy, and ambiguity properties of a given waveform with respect to range and Doppler can be characterized through its wideband ambiguity function [11], [7]. An example of such a function is shown in Fig. 1. An extensive analysis of a number of waveforms relevant to LFAS is presented by Collins [12]. He advises on how to interpret an ambiguity function, especially in the presence of reverberation. Experimental results for reverberation suppression using advanced pulses can be found in [13].

The method we propose consists in transmitting a Doppler-insensitive waveform with a range resolution sufficient to collect a quantity of contacts; see also [14]. A Doppler-sensitive waveform is then transmitted and its echoes processed only within a range and bearing bracket around the location of the contacts. The HFM contacts are then matched with the BPSK contacts and classified by means of their estimated range rate. This method requires a Doppler-sensitive pulse with a range resolution sufficient to allow the matching of the contacts of the Doppler-sensitive with that of the Doppler-insensitive waveform.

A. A Zoo of Pulses

The referenced Doppler-sensitive pulse in ASW is a long CW pulse [7], but its range resolution is insufficient for our application. Waveforms performance in the presence of reverberation and noise is characterized by their bandwidth-duration product (BT) [6]. The possibility to send waveforms exhibiting a high BT product at a high source level was limited by transducer technology, but developments in sensor technology [15] allow to transmit such pulses at frequencies relevant for LFAS.

Broadband Doppler-sensitive pulses can be classified in two classes according to their spectrum.

1) Comb Spectrum Pulses: Pulses such as the *Cox Comb* (a sum of sinusoids) [16], [7] or the pulse train of frequency modulation (PTFM, a series of short FM pulses) [13], [17] have a spiky spectrum that can be engineered so that the sidelobes in the Doppler direction are pushed to frequencies corresponding to a much higher Doppler than that of the reverberation at usual tow speeds. Despite their large bandwidth and their reverberation rejecting power, these pulses have a range resolution and accuracy only slightly better than that of a CW pulse of the same duration and their contacts are similarly difficult to associate with HFM contacts. Apart from Comb spectrum pulses, which have CW-like properties although performing better in heavy reverberation, also smooth spectrum wideband Doppler sensitive pulses exist.

2) Smooth Spectrum Pulses: Smooth spectrum pulses are attractive since they offer the "ideal" ambiguity function, combining a high range resolution (comparable to HFM) and high Doppler resolution (comparable to CW). However, the high sidelobe levels in their response functions are a limiting factor to their performance in heavy clutter environments.

Examples of pulses in this class are pseudorandom pulses [7], [18], [19] such as Costas pulses [20]. They consist of a collection of short CW pulses at different frequencies cleverly arranged in "Costas arrays" [21] so as to minimize sidelobes in the ambiguity function. Costas waveforms provide suitable range and Doppler resolution for our application but their ambiguity surfaces have spurious sidelobes that are problematic in heavy reverberant environments. Although these sidelobes can be predicted [22], they are undesirable and might cause false detections.

Other pulses in this class are phase-modulated waveforms such as the BPSK pulse. They provide a high range and Doppler resolution, but feature a flat *plateau* of sidelobes without outliers [22]. We will now examine the properties of this waveform in detail.

B. BPSK Pulse

The characteristics and performance of BPSK pulses for sonar detection have been developed by Jourdain in her founding work on semirandom pulses and their ambiguity surfaces [23], [24], [22]. BPSK pulses have been used for a variety of sonar applications [25], [26] as well as for underwater communications [27].

A BPSK waveform is constructed by modulating the phase of a sinusoidal carrier of frequency f_c transmitted for a duration T. A pseudorandom binary sequence $b(t)$ of N bits of duration T/N with good autocorrelation properties such as a maximum length pseudonoise sequence [24] is chosen. Every bit change is coded by applying a phase jump of π to the carrier, as shown in Fig. 2

$$s(t) = \sin(2\pi f_c\, t(2b(t) - 1)). \tag{1}$$

The 3-dB bandwidth of the resulting waveform is

$$B = \frac{N}{T} \tag{2}$$

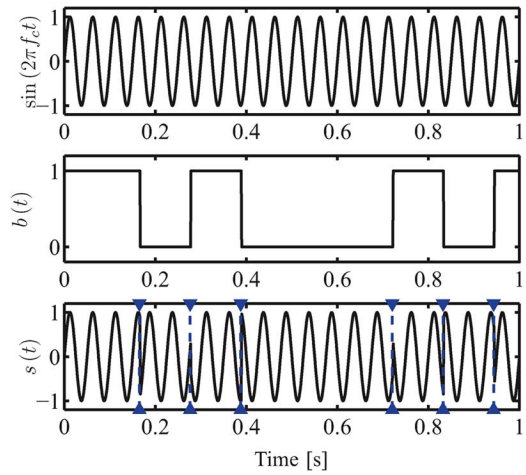

Fig. 2. Construction of a BPSK signal. Top: Carrier. Middle: pseudorandom bit sequences. Bottom: phase-modulated carrier; the triangles and dashed lines denote the phase jumps.

and its BT product is therefore equal to the number of bits in the sequence.

The full 3-dB Doppler resolution in meters per second of such a pulse [23] is

$$\delta_v \approx \frac{c}{f_c T} \tag{3}$$

where c is the speed of sound in water in meters per second. This happens to be the same as that of a CW waveform of the same length [8, p. 195]. Its full range resolution is

$$\delta_r \approx \frac{c}{2B} \tag{4}$$

which is the same as that of an HFM waveform of the same bandwidth. Hence, the BPSK waveform combines the advantages of both the CW pulse and the HFM pulse in terms of Doppler and range resolutions. This benefit comes at the price of a high sidelobe level (SLL), as can be seen in its wideband ambiguity function shown in Fig. 1. [The BPSK waveform used to compute that function is representative of the pulses used in LFAS sonars (pulse length 4 s, bandwidth 480 Hz, and number of bits 2047).] However, the sidelobe level is relatively constant, without outliers, and its average level is [23]

$$\text{SLL} = -10\log_{10}(N). \tag{5}$$

This constant level reduces the probability of false alarms due to sidelobes.

C. Limitations of the BPSK Waveform

1) High Data Volume: From the above, it may appear that the BPSK is the "ideal" sonar pulse and since it has existed already for quite some time, the question is raised why it is not used more in sonar applications. There appear to be practical limitations to the use of BPSK pulses. The most evident ones are discussed below.

The high range and Doppler resolution for a given BT product of the waveform mean that the range-Doppler cell subjected to detection, either by a computer-aided detection algorithm or an operator, must be small. A typical 4-s LFAS BPSK waveform with a center frequency of 1500 Hz and a BT product of 2047 will provide a Doppler and range resolution of 0.25 m/s and 1.5 m, respectively. With a pulse repetition time of 30 s the maximum range of the sonar will be 22.5 km (15×10^3 range cells). With 60 Doppler channels from -15 m/s to $+15$ m/s and 360 beams, the data size for a single ping will be 324×10^6 range-bearing-Doppler cells (about 1.2 GB in single precision). This signal processing produces a volume of data tedious to handle with a desktop computer. Moreover, the detection process in the huge data cube is very similar to that of the proverbial needle and the haystack.

2) Sensitivity to Doppler Perturbation: As we saw in Section II-B, the BPSK waveform is very Doppler sensitive. This implies that its performance is likely to be affected by Doppler spreading. There are various causes for Doppler spreading such as propagation through a time-varying medium [28], [29], or a maneuvering extended target. To give a representative example, we will consider Doppler spreading due to the movement between the source and the receiver.

Towed acoustic sources are very practical for LFAS operations because they can be towed at any convenient depth depending on the environmental parameters at the actual time and their effect on acoustic propagation performance. However, they are subjected to hydrodynamic constraints originated by sea state or high tow speed. These can cause pendular oscillations of the towed body. In a dual tow configuration, a high sea state might give way to motion between the source and the towed array.

These oscillations result in a variation in the range between the source, a given scatterer, and the towed array, which translates into a distortion of the Doppler spectrum of a given echo. Depending on the nature of the distortion, the effect on the performance can be a bias on the Doppler estimate but also a spreading of the echo Doppler spectrum. The latter can reduce the signal-to-noise ratio and therefore affect the detection performance.

To assess the effect of such a perturbation, we simulated a worst case scenario in which the received echoes are affected by a Doppler spread. We assume that the range is affected by a sinusoidal perturbation (corresponding to the pendular movement of the source) such that a given echo contains both positive and negative Doppler shifts. The period of this sinusoidal perturbation (4 s) is chosen equal to the pulse length for simplicity and is close to a typical wave period (5–6 s [28]). The amplitude of the oscillation of the source is expected to be around a meter or less (observed through the equalization of communication signals), corresponding to a distortion amplitude (α) of about 0.7 ms. We simulated perturbations of an amplitude up to 1 ms to obtain the worse case scenario.

The perturbation amounts to the transform

$$p(t) \mapsto p_\alpha(t) = p\left(t + \alpha \sin 2\pi \frac{t}{T}\left(1 - \cos 2\pi \frac{t}{T}\right)\right) \tag{6}$$

where $p(t)$ is the pulse as a function of time, T is the pulse length, α is the amplitude of the distortion, and p_α is the distorted pulse.

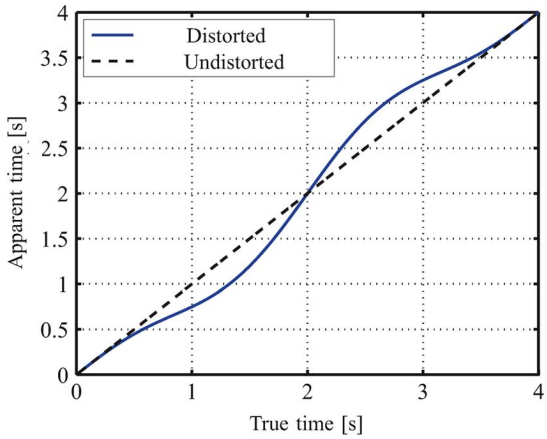

Fig. 3. Time distortion applied to a 4-s pulse with an amplitude of 0.5 s.

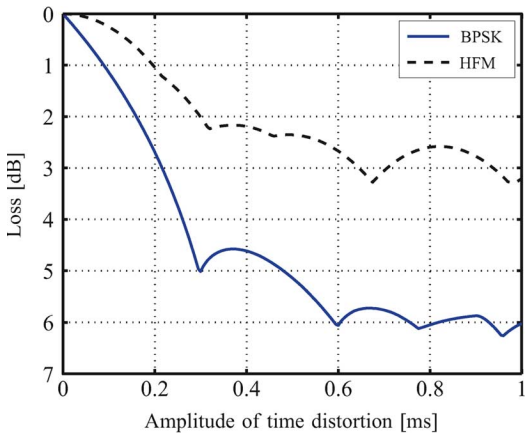

Fig. 4. Loss caused by time distortion on the range/Doppler responses of HFM and BPSK waveforms.

To simulate this effect, we interpolated a 4-s BPSK waveform (2047-b, 480-Hz bandwidth) on a distorted time vector (shown in Fig. 3) using (6) and then applied a Doppler-sensitive matched filter (similar to that used in our sonar processing chain) as follows:

$$\chi_\alpha(\tau, d) = \int_{-T/2}^{+T/2} p_\alpha(t) p(d(t-\tau)) dt \tag{7}$$

where τ is the time lag, and d is a Doppler time scale factor corresponding to a range rate U

$$d = \frac{c-U}{c+U}. \tag{8}$$

The maximum energy value of the resulting time Doppler matrix $\chi_\alpha(\tau, d)$ was then determined and plotted against the amplitude of the time distortion in Fig. 4. Range and Doppler cuts of the distorted pulses correlated with the clean replica are represented for three representative values of α in Fig. 5. Furthermore, we applied the same distortion and a Doppler-insensitive matched filter to a typical LFAS HFM waveform of the same duration and bandwidth and plotted the degradation in Fig. 4. The cross correlation of the distorted HFM waveform with the clean replica is plotted in Fig. 5 as well. This simulation shows that the level of a BPSK echo can be heavily degraded (down to 6 dB) by a Doppler spread while the HFM echo remains almost unaffected with a maximum loss around 3 dB. This result is far from surprising as HFM pulses have been designed to be Doppler insensitive [30]. The effect of the perturbations can also be observed in the resulting Doppler estimate. From the lower row of Fig. 5, one can see that these result in both a spread in the mainlobe and a bias in the Doppler estimate. This spread signifies that the standard deviation of the accuracy of the Doppler estimate will most likely be increased.

These deficiencies of the BPSK waveforms help emphasize the point that for an application such as ASW, one cannot rely entirely on a highly range- and Doppler-sensitive waveform such as BPSK, as the volume of data is cumbersome, and the pulse may be heavily affected by Doppler spreading. However, a BPSK echo provides an accurate measurement of a contact's Doppler in one ping, which can quickly help classify many false alarms in an ASW sonar picture in heavily reverberating environments.

III. Experimental Results

A. Experiment Description

An experiment in which HFM and BPSK pulses were transmitted alternately was carried out during the 2005 Netherlands Low Frequency Active Sonar (NL-LFAS 2005) trial in Norwegian waters near Stavanger. *Hr. Ms. Mercuur* (MER) towed the interim removable low-frequency active sonar system (IRLFAS) [2], which has a wideband source and a port-starboard ambiguity resolving receiver. The target was a Walrus class submarine (SUB). MER was sailing a straight southward track while SUB was varying its range at different rates as shown in Fig. 6.

The experiment was performed in a particular North Sea environment. The morphology and nature of the sea bottom were different on port and starboard. The submarine on starboard sailed over the flanks of a sandy hill. The area on port, between the hill and the coastline, was a relatively flat muddy plain. The nautical chart (Fig. 6) reports obstructions as well as a seamount with 150-m depth on this side.

The sound-speed profile was downward refracting, which means that heavy bottom interaction was encountered for propagating sound.

B. Experimental Ambiguity Function

The quality of the measured data and processing chain was assessed by comparing the measured range/Doppler surface of a given echo with the theoretical wideband ambiguity function of the transmitted waveform. In Fig. 7, we show such a surface, and in Fig. 8, we show cross sections in the Doppler and range directions. The echo is affected by a Doppler spread that degrades the actual Doppler resolution of the echo and the mainlobe-to-sidelobe ratio. Nevertheless, the mainlobe-to-sidelobe ratio as well as the signal-to-noise-and-reverberation ratios are more than sufficient to detect and classify the target.

C. Signal Processing

HFM and BPSK pings were transmitted in turns. The HFM echoes were first normalized in the range direction using a trend

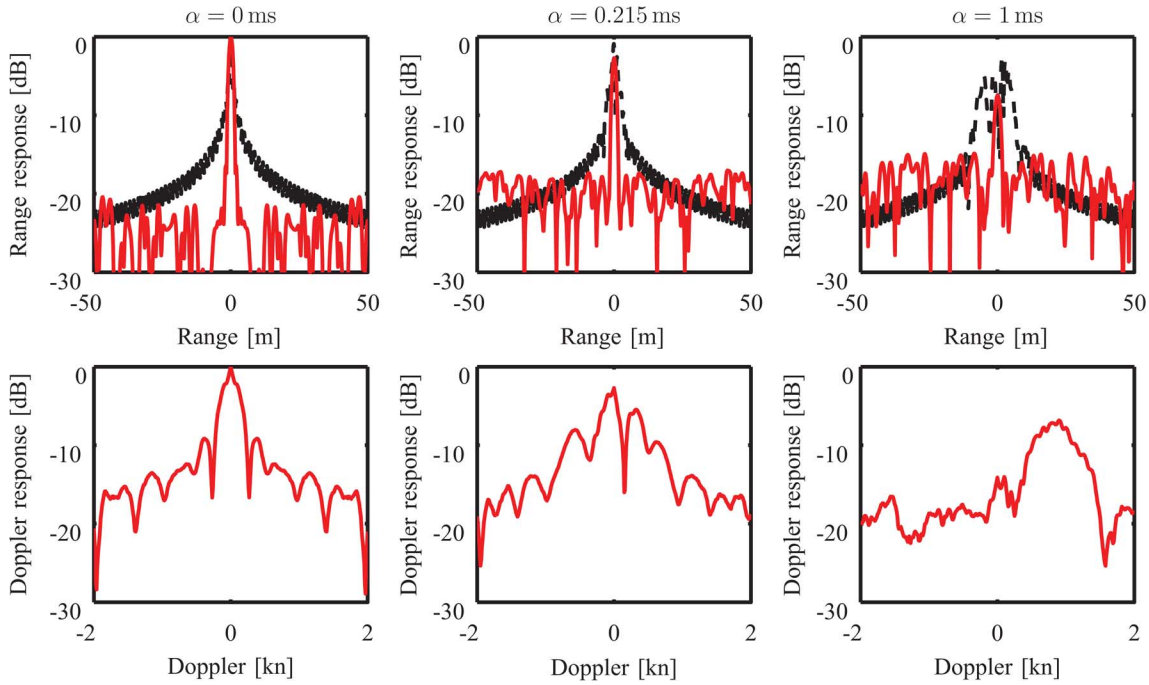

Fig. 5. Range response (top) for a distorted BPSK pulse (red continuous line) and an HFM pulse (black dashed line) and Doppler response for a distorted BPSK pulse for three distortion amplitudes: $\alpha = 0$ ms (left), $\alpha = 0.215$ ms (middle), and $\alpha = 1$ ms (right).

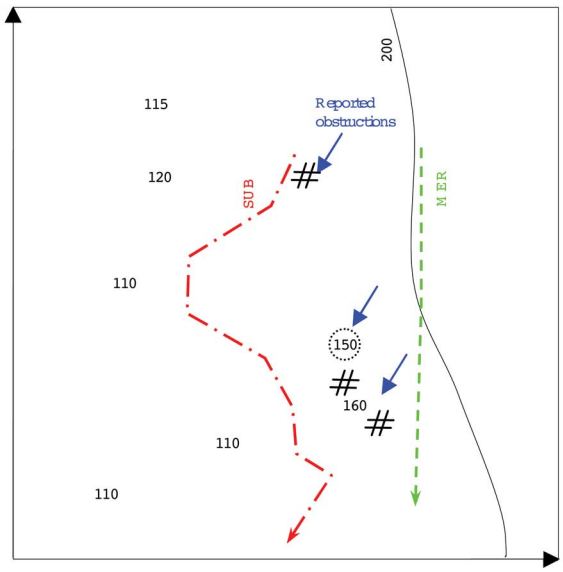

Fig. 6. The 2005 experiment sailed track on a nautical chart. The submarine and sonar platform tracks are plotted in red mixed line and green dashed line, respectively. The numbers indicate the bathymetry in meters.

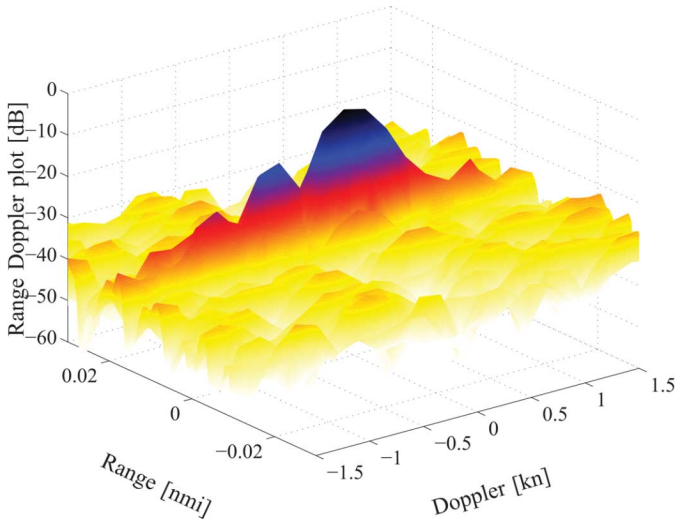

Fig. 7. Measured ambiguity surface (range/Doppler plot) of a BPSK echo (2047-b, 480-Hz bandwidth and 4-s pulse length).

removal highpass filter. A threshold was then applied to the signal to form contacts. These contacts were then fed to a classifier, which rejected a number of contacts, based on the features such as shape, size, or energy [5]. The location of the remaining HFM contacts was then stored and the BPSK matched filtering of the following ping was only performed in a narrow sector containing the location of these contacts.

A maximum search was then performed in a range-bearing-Doppler data cube centered on the geographical location of each HFM contact. The BPSK contacts originating from SUB and clutter were stored separately (with the help of the measured position of the submarine). The analysis described in Section III-E was performed on these BPSK contacts. This way of processing is significantly less memory and central processing unit (CPU) demanding than applying the Doppler-sensitive matched filter to the whole ping data. Moreover, it reduces the volume of data in which the BPSK detection is performed. This way of processing BPSK pulses is very similar to Alinat's work [14].

D. *Effect of Topography on Classification Performance*

In Fig. 10, the location of all BPSK LFAS contacts of the whole experiment is shown in a range-bearing plot. The target

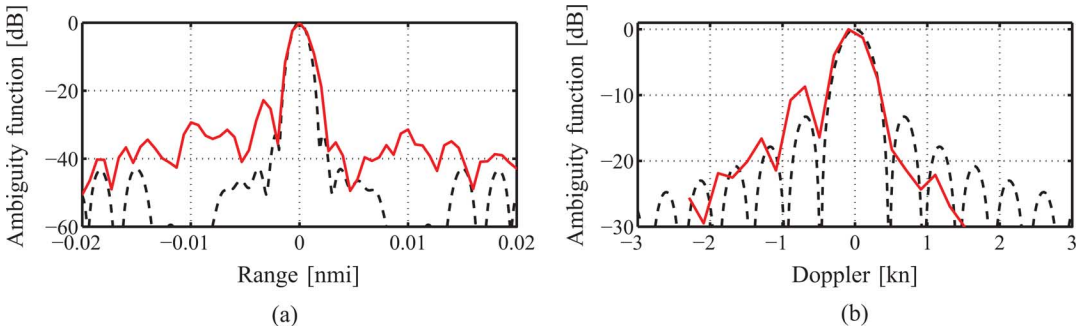

Fig. 8. Measured (red solid line) and ideal (black dashed line) (a) range and (b) Doppler responses measured as cross section of the ambiguity function of a measured echo of a BPSK waveform.

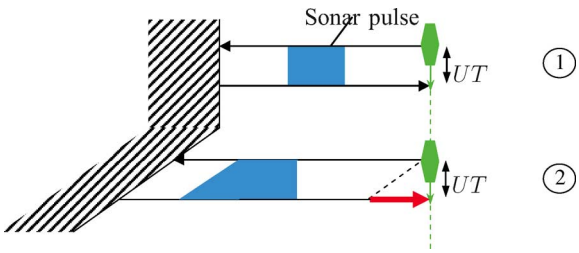

Fig. 9. Nonspecular reflection by an angled reflector. In (1), the reflector is parallel to the transceiver path, and the range of the scatterer does not change within the pulse duration. In (2), the range of the scatterer changes between the instants the sonar pulse begins and finishes to insonify the scatterer. The pulse received by the receiver does not have the same length as the pulse it transmitted. Judging from the Doppler, the echo appears to belong to a moving target.

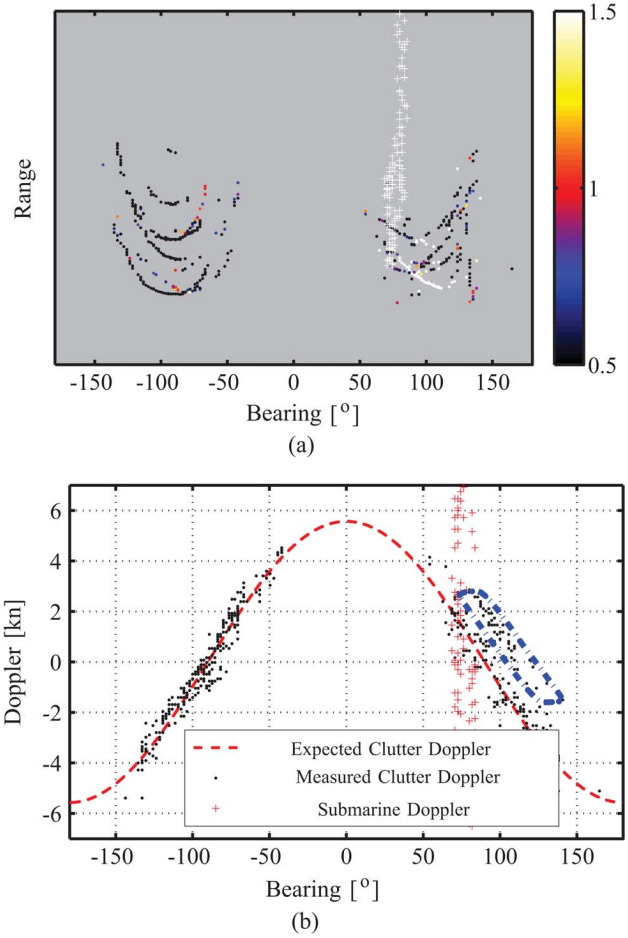

Fig. 10. BPSK contacts collected during the 2005 experiment. (a) Range/bearing plot of the contacts; the color symbolizes the absolute Doppler in knots as defined in (9). The submarine contacts are represented by a +. (b) Doppler-bearing plot of the contacts. The blue mixed line contains a group of contacts exhibiting a particular Doppler value.

track (first sailing out and then closing in) is visible on starboard bearings between 70° and 90°. In Fig. 10, a cluster of contacts indicated by a dashed contour is detached from the rest of the clutter contacts. These contacts exhibit a Doppler value that would lead to thinking that they originated from a moving object. The presence of another moving large scatterer in the area being improbable, this echo was very likely to be clutter related. The origin of this structure is investigated in the following.

The position of this contact structure corresponds to the obstructions signaled in the nautical chart by blue arrows and a steep ridge in this area. This ridge is at an angle compared to the track of the platform. As explained in Fig. 9, a strong extended scatterer positioned at an angle compared to the platform track can generate a contact displaying a Doppler different from that of the clutter in that bearing. The most likely explanation for this contact structure is then an angled ridge or an oil pipe. Such a structure can give very strong specular echo. As shown in Fig. 9, this kind of configuration can result in an echo being affected by a time stretch while the echo itself is not moving. A very trivial analogy is that of a car driving along a continuous mirror surface. If the surface is parallel to the trajectory of the car, it gives the impression of observing a car driving side by side with oneself. However, if the surface is at an angle compared to the car trajectory, one will have the impression that one's reflection is driving away from or towards oneself. In sonar, this kind of configuration results in an apparent Doppler and could not be resolved with a multiple target tracker as the apparent range rate corresponds to the variation in range of the reflector.

E. Classification Results

To assess the classification performance with the BPSK waveform, we analyzed the statistics of the measured Doppler of clutter originated contacts. Let the "absolute Doppler" of each contact be

$$\dot{r}_{abs} = \dot{\tilde{r}} - U(t)\cos\varphi \tag{9}$$

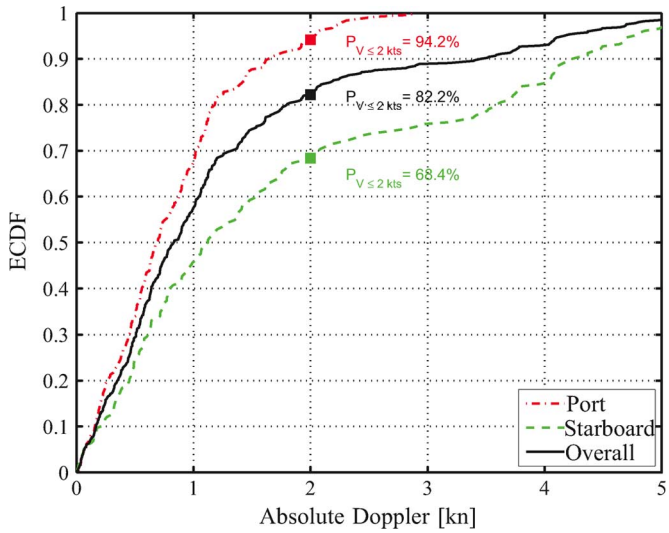

Fig. 11. ECDF of the absolute Doppler of all the BPSK contacts exceeding a preset signal-to-noise ratio threshold collected over the whole experiment.

where $U(t)$ is the towship speed, and $\tilde{\dot{r}}$ and φ are the measured Doppler and bearing of each contact, respectively. If an object is still on a flat bottom, its "absolute Doppler" will be null. The reciprocal is not always true. Indeed, a moving object might have a zero "absolute Doppler" in certain conditions, for instance, when the object is sailing along side the sensor at the same speed and in a broadside bearing. Apart from these particular configurations, the "absolute Doppler" is a good candidate feature for determining whether an object is moving.

However, absolute Doppler estimates are corrupted by measurement errors, propagation effects, unwanted sonar motion as well as the other effects shown in Fig. 9.

To assess the performance of the transmitted waveform and its associated processing as a classifier, we removed the contact corresponding to the submarine from each ping and collected all the clutter-related contacts over the whole experiment. The absolute Doppler of each contact was then computed, as well as the empirical cumulative density function (ECDF) of the absolute Doppler of all the BPSK contacts collected over the whole experiment. The ECDF gives an *a posteriori* probability of correct classification as a nonmoving object. This function for this data set is plotted in Fig. 11 for port, starboard, and both sides. For instance, we see that with an absolute Doppler threshold of 2 kn, 68.4% of the contacts are correctly classified as nonmoving object on the starboard side, 94.2% on port, and 82.2% overall. The difference in classification performance between port and starboard is due to the topographic structure mentioned in Section III-D.

IV. Summary and Conclusion

The Doppler-sensitive BPSK pulse for LFAS was studied. BPSK is a pseudorandom wideband pulse that originates from communication applications. A conceptual comparison with other LFAS waveforms in terms of performance shows that this pulse has potential for LFAS applications. The BPSK's response shows high resolution in range and Doppler, which means that targets can be accurately localized and classified (based on Doppler) with one pulse.

This theoretical performance is formalized and confirmed with simulated results. It gives the impression of a quasi-ideal pulse. Its ambiguity surface shows both a remarkably high resolution in range and Doppler. Moreover, the ambiguity surface sidelobes levels are flat (though high), whereas other wideband Doppler-sensitive pulses show a more unpredictable sidelobe behavior.

Several experiments at sea were performed with BPSK pulses insonifying submarines. One of these experiments (off Norway) was analyzed, in complicated propagation conditions and high reverberation levels. A solution was found to avoid the fact that these wideband pulses are computationally expensive to process leading to a robust implementation in the semi-operational IRLFAS system.

A simulation study confirmed the idea that Doppler spread due to sonar motion and propagation may be the cause of the performance loss.

The accurate Doppler estimation of the BPSK pulse enables good classification possibilities to separate clutter-like reverberation from moving submarines, and can be used as a classification tool as long as detection is being performed with another pulse (FM). Its false-alarm reduction capability by Doppler analysis is complementary to that of the echo-cluster analysis in FM-only mode. This classification power can substantially reduce the number of false contacts (82.2% in the analyzed experiment) in LFAS applications in heavy clutter areas. However, it should be noted that the topography can influence the measured clutter Doppler and that information from a nautical chart or bathymetric map can help resolve more false alarms. Further research that would bring even more insight on the performance of BPSK is the evaluation of the performance of the HFM–BPSK combination at the tracker level as performed in [9] and [10] and its comparison to the performance of HFM–CW or HFM–PTFM combinations.

Acknowledgment

The authors would like to thank Dr. van Walree, Dr. Blacquière, and Dr. van Vossen as well as Ing. van de Spek and Prof. Simons for their useful comments. The experiments mentioned in this paper were carried out thanks to A. Gerk, Ing. van Ijsselmuide, Ing. Janmaat, and Ing. van Spellen and The Netherlands Royal Navy Submarine Service. The authors would like to thank the reviewers for their constructive comments that helped make this paper clearer and more accurate.

References

[1] G. Tyler, "The emergence of low-frequency active acoustics as a critical antisubmarine warfare technology," *Johns Hopkins APL Tech. Dig.*, vol. 13, no. 1, pp. 145–159, 1992.

[2] S. P. Beerens and E. van der Spek, "The interim removable low frequency active sonar system," in *Proc. Eur. Conf. Undersea Defence Technol.*, 2006, Session 3A-1, CD-ROM.

[3] O. Gerard, S. Coraluppi, C. Carthel, and D. Grimmett, "Benchmark analysis of NURC multistatic tracking capability," in *Proc. 9th Int. Conf. Inf. Fusion*, Jul. 2006, vol. 1, DOI: 10.1109/ICIF.2006.301698.

[4] P. A. M. de Theije, L. Kester, and J. Bergmans, "Application of the M6T tracker to simulated and experimental multistatic sonar data," in *Proc. 9th Int. Conf. Inf. Fusion*, 2006, DOI: 10.1109/ICIF.2006.301799.

[5] S. P. Beerens and W. Boek, "A robust algorithm for LFAS target classification," in *Proc. Undersea Defence Technology Eur.*, 2007, vol. 1, p. 1, Session 6C-3, CD-ROM.
[6] Y. Doisy, L. Deruaz, S. P. Beerens, and R. Been, "Target doppler estimation using wideband frequency modulated signals," *IEEE Trans. Signal Process.*, vol. 48, no. 5, pp. 1213–1224, May 2000.
[7] T. Collins and P. Atkins, "Doppler-sensitive active sonar pulse designs for reverberation processing," *Inst. Electr. Eng. Proc.—Radar Sonar Navig.*, vol. 145, no. 6, pp. 347–353, Dec. 1998.
[8] X. Lurton, *An Introduction to Underwater Acoustics: Principles and Applications*. New York: Springer-Verlag, 2002.
[9] C. Rago, P. Willett, Y. Bar-Shalom, S. Syst, and M. Woburn, "Detection-tracking performance with combined waveforms," *IEEE Trans. Aerosp. Electron. Syst.*, vol. 34, no. 2, pp. 612–624, Apr. 1998.
[10] Y. Sun, P. Willett, and R. Lynch, "Waveform fusion in sonar signal processing," *IEEE Trans. Aerosp. Electron. Syst.*, vol. 40, no. 2, pp. 462–477, Apr. 2004.
[11] D. Swick, "An ambiguity function independent of assumptions about bandwidth and carrier frequency," Naval Res. Lab., Washington, DC, Tech. Rep., 1966.
[12] T. Collins, "Active sonar pulse design," Ph.D. dissertation, Faculty Eng., Univ. Birmingham, Birmingham, U.K., 1996.
[13] Y. Doisy, L. Deruaz, S. P. van IJsselmuide, S. P. Beerens, and R. Been, "Reverberation suppression using wideband Doppler-sensitive pulses," *IEEE J. Ocean. Eng.*, vol. 33, no. 4, pp. 419–433, Oct. 2008.
[14] P. Alinat and G. Bienvenu, "Signal-processing method and active sonar implementing same part of the signal received corresponding to the second pulses for the alarms satisfying at least one predetermined criterion," U.S. Patent 7 355 925, Apr. 8, 2008.
[15] J. Zalesak and P. Rogers, "Low-frequency radiation characteristics of free-flooded ring transducers with application to a low-frequency directional hydrophone," *J. Acoust. Soc. Amer.*, vol. 56, no. 4, pp. 1052–1058, 1974.
[16] H. Cox and H. Lai, "Geometric comb waveforms for reverberation suppression," in *Proc. 28th Asilomar Conf. Signals Syst. Comput.*, Oct.–2 Nov. 1994, vol. 2, pp. 1185–1189.
[17] S. P. Van IJsselmuide, S. P. Beerens, Y. Doisy, and L. Deruaz, "New sonar waveform for active torpedo warning using an LFAS system," in *Proc. Undersea Defense Technol.*, 2003, Session 3A-3, CD-ROM.
[18] S. Pecknold, "Ambiguity and cross-ambiguity properties of some reverberation suppressing waveforms," Defence R&D Canada Atlantic, Tech. Rep, 2002.
[19] B. Flores, E. Solis, and G. Thomas, "Assessment of chaos-based fm signals for range Doppler imaging," *Inst. Electr. Eng. Proc.—Radar Sonar Navig.*, vol. 150, no. 4, pp. 313–22, Aug. 2003.
[20] J. Costas, "A study of a class of detection waveforms having nearly ideal range-Doppler ambiguity properties," *Proc. IEEE*, vol. 72, no. 8, pp. 996–1009, Aug. 1984.
[21] S. Golomb and H. Taylor, "Constructions and properties of costas arrays," *Proc. IEEE*, vol. 72, no. 9, pp. 1143–1163, Sep. 1984.
[22] J. Millet and G. Jourdain, "Signaux à fort pouvoir de résolution temps-fréquence: Comparaison entre les signaux de costas et les signaux à modulation binaire de phase (B.P.S.K.)," *Traitement du Signal*, vol. 7, no. 1, pp. 27–40, 1990.
[23] G. Jourdain, "Considérations sur la fonction d'ambiguité dans le cas de signaux aléatoires: Étude et génération de certains de ces signaux," Ph.D. dissertation, Faculté des Sciences, Université de Grenoble, Grenoble, France, 1970.
[24] G. Jourdain and J. Henrioux, "Use of large bandwidth-duration binary phase shift keying signals in target delay Doppler measurements," *J. Acoust. Soc. Amer.*, vol. 90, no. 1, pp. 299–309, 1991.
[25] C. Eggen and R. Goddard, "Bottom mounted active sonar for detection, localization, and tracking," in *Proc. MTS/IEEE OCEANS Conf.*, Oct. 2002, vol. 3, pp. 1291–1298.
[26] K. Nakahira, S. Okuma, T. Kodama, and T. Furuhashi, "The use of binary coded frequency shift keyed signals for multiple user sonar ranging," in *Proc. IEEE Int. Conf. Netw. Sens. Control*, 2004, vol. 2, pp. 1271–1275.
[27] M. B. van Gijzen and P. A. van Walree, "Shallow-water acoustic communication with high bit rate BPSK signals," in *Proc. MTS/IEEE OCEANS Conf. Exhib.*, 2000, vol. 3, pp. 1621–1624.
[28] P. van Walree, T. Jenserud, and M. Smedsrud, "A discrete-time channel simulator driven by measured scattering functions," *IEEE J. Sel. Areas Commun.*, vol. 26, no. 9, pp. 1628–1637, Dec. 2008.
[29] J. Hermand and W. Roderick, "Delay-Doppler resolution performance of large time bandwidth- product linear FM signals in a multipath ocean environment," *J. Acoust. Soc. Amer.*, vol. 84, no. 5, pp. 1709–1727, 1988.
[30] J. Kroszczynski, "Pulse compression by means of linear-period modulation," *Proc. IEEE*, vol. 57, no. 7, pp. 1260–1266, Jul. 1969.

Mathieu E. G. D. Colin received the M.Sc. degree in electronic engineering from the Ecole Nationale Superieure des Ingénieurs des Etudes et Techniques de l'Armement (ENSIETA), Brest, France, in 2001. Currently, he is working towards the Ph.D. degree underwater acoustics in the Faculty of Aerospace Engineering, Delft University of Technology, Delft, The Netherlands.

Since 2001, he has worked at the Sonar Department, The Netherlands Organization for Applied Research (TNO), The Hague, The Netherlands, on sonar related topics such as active and passive sonar processing applied to towed array and diver detection sonars.

S. Peter Beerens graduated in theoretical physics from the University of Amsterdam, Amsterdam, The Netherlands, in 1990, after which he pursued a Ph.D. study on chaotic mixing behavior in tidal areas at the Royal Netherlands Institute for Sea Research, Texel, The Netherlands. He received the Ph.D. degree in physics from Utrecht University, Utrecht, The Netherlands, in 1995.

Currently, he works in the undersea research at The Netherlands Organization for Applied Scientific Research (TNO), The Hague, The Netherlands. He is a Senior Scientist and Program Manager in the Sonar Department, TNO. He specializes in sonar signal processing and sea trials. He has worked on several topics in underwater acoustics, such as low-frequency active sonar (LFAS), submarine sensors, diver detection sonar, and bioacoustics. Currently, his main interests are in LFAS applications and new sonar waveforms.